CYCLIC OXIDATION BEHAVIOR OF $\beta+\gamma$

OVERLAY COATINGS ON γ AND $\gamma+\gamma'$ ALLOYS

J. A. Nesbitt*, B. H. Pilsner, L. A. Carol and R. W. Heckel
Michigan Technological University
Houghton, Michigan 49931
USA

Summary

Detailed experimental studies of the cyclic oxidation behavior of low-pressure plasma sprayed $\beta+\gamma$ coatings on γ-phase Ni-Cr-Al alloys have shown the correlation of weight change, oxide type, and Cr and Al concentration-distance profiles as a function of oxidation time. Of special interest was the transition to breakaway oxidation due to the loss of the Al flux to the oxide and the failure of the coated alloy to form an Al_2O_3-rich oxide scale. The experimental results on $\beta+\gamma/\gamma$ coating systems were used as the basis of a numerical model (ternary, semi-infinite, finite-difference analysis) which accurately predicted changes in Cr and Al concentration-distance profiles. The model was used to study parameters critical to enhancing the life of coatings which fail by a combination of Al loss in forming the oxide scale and Al loss via interdiffusion with the substrate alloy. Comparisons of $\beta+\gamma/\gamma$ coating behavior are made to the oxidation of coated $\gamma+\gamma'$ substrates, both ternary Ni-Cr-Al alloys and Mar-M 247-type alloys.

*Currently at National Aeronautics and Space Administration, Lewis Research Center, Cleveland, Ohio 44135.

Introduction

Overlay coatings provide an improved means for imparting oxidation resistance to superalloy components (1-6); specific coating compositions can be applied in order to provide maximum environmental protection to the underlying superalloy which has a composition/structure designed to withstand applied stress conditions. Such a view of the coating/substrate system is based upon the premise of minimal coating degradation by either the oxidation protection mechanism or interaction with the superalloy substrate. Such degradation mechanisms could be operative in the high-temperature operating regimes of the coated superalloy.

The cyclic oxidation behavior of as-cast, $\beta+\gamma$, Ni-Cr-Al (with small amounts of Zr) alloys was investigated earlier (7,8). These studies correlated the cyclic-oxidation weight change as a function of time (paralinear), the type of the oxide formed, and the microstructure and concentration-distance profiles of Ni, Cr and Al near the forming/spalling oxide layer. Of particular interest in these studies was the nature of the γ layer which grows adjacent to the oxide (loss of Al-rich β due to the formation of Al_2O_3-rich oxides). The γ layer thickened via the diffusion of Al from the $\gamma/\beta+\gamma$ interface to the γ/oxide interface and Cr and Ni diffusion in the reverse direction, with Ni diffusing up its concentration gradient. The progressive loss of Al from the coating shifted the concentration-distance profiles across the phase diagram, resulting in increasing Al concentrations in the γ at the $\gamma/\beta+\gamma$ interface. More importantly, the Al concentrations at the γ/oxide interface decreased with time. These changes in Al concentration with time at the $\gamma/\beta+\gamma$ and γ/oxide interfaces during γ-layer growth resulted in an Al gradient at the γ/oxide interface which was essentially time independent during the formation of Al_2O_3-rich oxides. The constancy of the Al gradient resulted in a constant Al flux (assuming no Al flux due to the Cr gradient), in accord with the almost constant rate of weight loss of the sample due to oxide spallation.

Breakaway oxidation, rapid weight loss during later stages of cyclic oxidation due to the formation of less protective oxides (e.g., NiO), was found to occur as the Al concentration at the γ/oxide interface neared zero. Following this point in the oxidation process, the Al gradient decreased with time, curtailing the delivery of Al in amounts necessary to sustain the continued formation of an Al_2O_3-rich oxide layer. Thus, breakaway oxidation may be defined in terms of accelerated weight loss, formation of nonprotective oxides, and the marked reduction in the Al gradient in the γ phase at the γ/oxide interface as the Al concentration nears zero at this location.

The present investigation was designed to provide an understanding of the interdependence of Al diffusion necessary to provide oxidation protection via Al_2O_3-rich oxide formation and Al diffusion into the superalloy substrate. The study was aimed primarily at four γ-phase Ni-Cr, Ni-Al, and Ni-Cr-Al alloys which had been low-pressure plasma sprayed with a $\beta+\gamma$ Ni-Cr-Al-Zr coating. Cyclic oxidation testing provided weight change data, oxide type, and specimens for microstructure and electron microprobe analysis as a function of oxidation time. The second main thrust of the investigation was the development of a mathematical diffusion model which would predict both the Al and Cr concentration-distance profiles as a function of oxidation time for $\beta+\gamma$ coatings on γ substrates and, thereby, predict coating life (time to breakaway oxidation, as defined by an Al concentration of zero at the γ/oxide interface). In addition, the investigation was to compare $\beta+\gamma/\gamma$ behavior to $\beta+\gamma/\gamma+\gamma'$ behavior. To this end, $\gamma+\gamma'$ substrates formed from Ni-Cr-Al and Mar-M 247-type alloys were investigated.

Procedure

The compositions of the four γ-phase alloys and the β+γ coating composition used throughout the study are shown in Table I.

Table I. Alloy and Coating Compositions

Nominal Composition	Actual Composition (atomic percent) Cr	Al	Zr
Alloys			
Ni-10Cr	11.7	-	-
Ni-10Al	-	6.7	-
Ni-20Cr	22.6	-	-
Ni-10Cr-10Al	11.5	7.0	-
Coating			
Ni-13Cr-25Al	13.5	24.9	0.05

The alloys were prepared by arc melting (numerous remelting steps) in a button melter. The coating was applied by low-pressure plasma spraying on 0.63 cm. diameter, 2.54 cm. length specimens. As-deposited coatings were typically 50-100 μm thick. Coated specimens were annealed at 1150°C for two hours (in argon) prior to oxidation testing.

Oxidation testing was carried out in air at 1150°C for cycles of one hour at temperature followed by a 20 min. cooling period. Weight change data were determined as a function of time along with the structure of the oxide.

Ternary diffusion coefficient data were necessary for the development of the mathematical model. A variety of γ and β+γ compositions (binary and ternary Ni-Cr-Al alloys) were arc melted and bonded/interdiffused in a Mo container which caused bonding by differential thermal expansion. Diffusion treatments were carried out at 1100 and 1200°C, providing specimens for electron microprobe analysis to obtain D_{AlAl}, D_{AlCr}, D_{CrCr} and D_{CrAl} and their activation energies as a function of composition throughout the γ phase field.

Electron microprobe analysis was carried out using the MULTI8 ZAF correction program (9). Comparisons of probe analyses of seven γ-phase standards indicated that accuracies were approximately ±0.4a/o Al, ±0.6a/o Cr and ±2.0a/o Ni. Microprobe analysis was carried out both on oxidized coated specimens and diffusion couples.

Results

An example of weight change time data for cyclic oxidation is shown in Figure 1 for the Ni-10Cr alloy. (Compositions will be given in nominal atomic percent throughout this paper.) The other substrates developed the more-normal constant negative slope after the initial parabolic increase in weight. The magnitude of the negative slope increased in the order Ni-10Al, Ni-20Cr, Ni-10Cr-10Al. The COSP spalling model curve shown in Figure 1 was

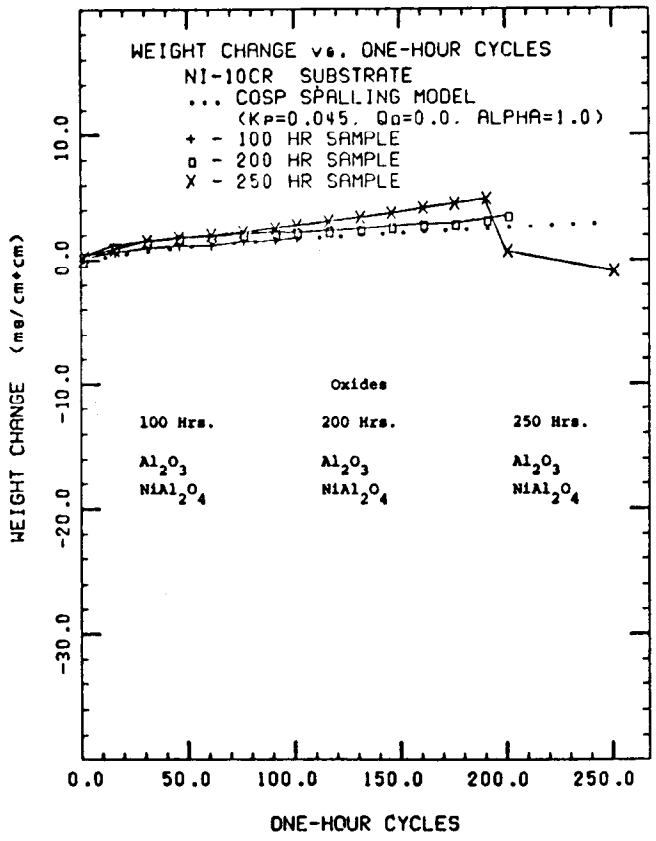

Figure 1. - Weight change during cyclic oxidation for three specimens (tests terminated at 100, 200 and 250 hours) with a Ni-10 Cr substrate composition.

obtained from an analytical model (10) based upon parabolic oxide growth and cyclic spallation. Cyclic oxidation weight change data for each coated substrate were fitted to the COSP model to provide aluminum consumption rate data as a function of time to be used as a boundary condition for the mathematical model.

Concentration-distance profiles for both Al and Cr as determined by electron microprobe analysis are shown in Figure 2 for Ni-10Cr substrates (same specimens with weight change data given in Figure 1 plus a short-term, 10-hour oxidation specimen). It is particularly noteworthy that extensive interdiffusion takes place even at times as short as 10 hours; coatings on all substrate compositions underwent complete loss of the β phase within 5 to 15 hours of oxidation (or, approximately, only about 5-10% of the failure time (breakaway oxidation) of the coating). The rate of diffusional change is also shown by the loss of 60% of the Al in the coated layer during the first 10 hours of oxidation. Furthermore, the "active depth" of the coating (diffusion depth) is greater than five times the thickness of the original coating, with the maximum Al concentration occurring at depths of about two to three times the original coating thickness. It is also noteworthy that the coatings on Ni-10Cr and Ni-20Cr substrates exhibited variations in the Al gradient at the coating/oxide interface, a departure from the cyclic oxidation behavior of $\beta+\gamma$ alloys studied previously (7,8). This time-dependence of the Al gradient is due,

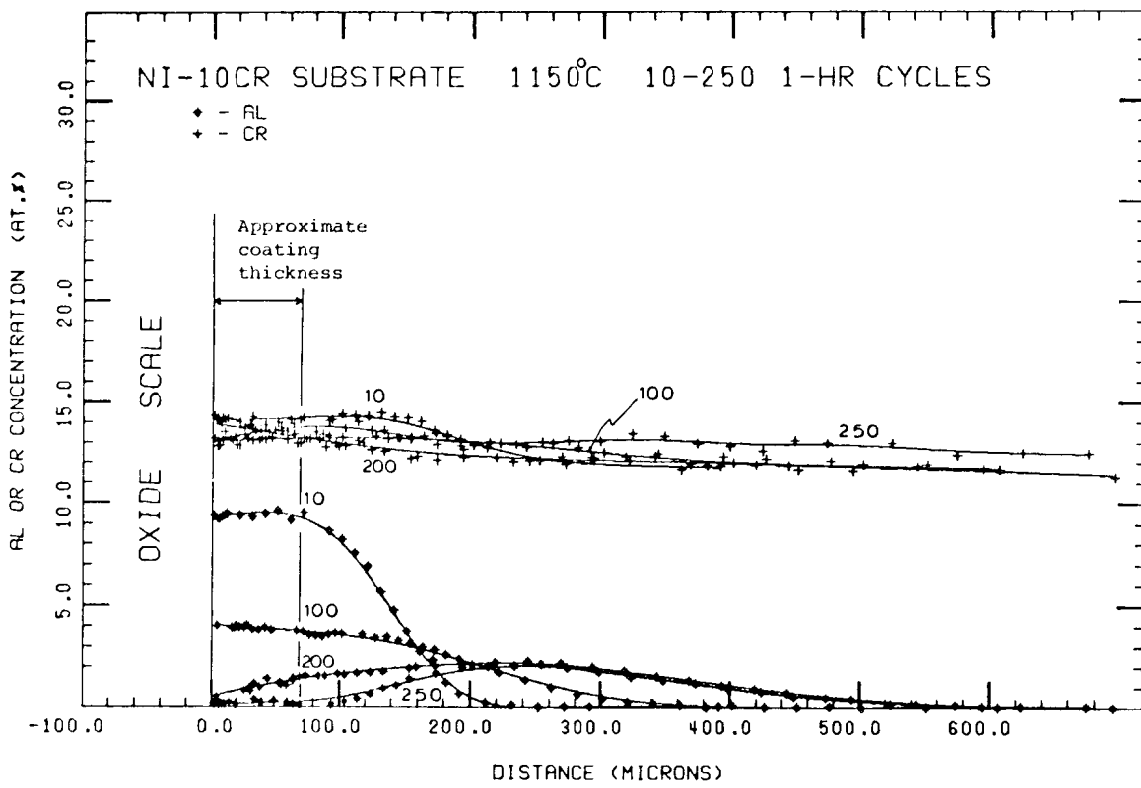

Figure 2. - Concentration-distance profiles for oxidized coatings (tests terminated at 10, 100, Ni-10Cr substrates.

primarily, to the rapid rate of inward diffusion of Al in the case of thin coatings on substrates without Al; the Ni-10Al and Ni-10Cr-10Al substrates in the present study generally exhibited negligible time-dependence in the Al gradient in the γ phase at the coating/oxide interface. Correspondence between breakaway oxidation parameters such as accelerated weight loss, change in surface oxide to NiO or Cr_2O_3, and essentially negligible Al concentration in the γ phase at the coating/oxide interface was generally found for all coated substrate compositions. (It is thought that the Ni-10Cr substrate for which data are shown, is very near the point of breakaway oxidation as judged by both the onset of erratic weight change data and the surface Al concentration, even though there was no evidence of the formation of nonprotective oxides at up to 250 hours of testing.)

The large number of diffusion couple alloy compositions that were used provide extensive experimental data for obtaining the ternary diffusion coefficients as a function of temperature (interdiffusion at 1100 and 1200°C; exponential interpolation for intermediate temperatures) and composition (essentially, the γ-phase field of about 0-12% Al and 0-40% Cr). Concentration-distance profiles for both Al and Cr were determined in the γ-phase region of γ/γ, $\gamma/\gamma+\beta$ and $\gamma/\gamma+\gamma'$ couples. Data analysis to provide diffusion coefficients was carried out by established methods (11-14). Regression analyses were used to provide the four ternary diffusion coefficients as functions of composition and temperature. The accuracy of the coefficients provided by the analysis was checked by comparison to back-calculated concentration-distance profiles (finite-difference techniques) for all of the couples which were studied experimentally. Differences between calculated and experimentally-determined concentration-distance profiles for both Al and Cr were generally equivalent to the accuracy range of the microprobe concentration measurements.

Discussion

A mathematical model to be used to predict diffusional phenomena, including the onset of breakaway oxidation, was developed on the basis of established finite-difference techniques (15) and boundary conditions found in the present investigation and prior studies (7,8). It was assumed that the coating, as well as the alloy, was single-phase γ since the β phase existed for only a small fraction of the coating life; diffusion coefficients for the high-Al, metastable, γ phase were obtained by extrapolation of the regression-analyzed γ-phase data. It was also assumed that all diffusion occurred at the oxidation temperature (1150°C), i.e., heating and cooling were rapid. The γ/oxide boundary condition was established by the COSP spalling model (10); predicted Al consumption rate as a function of time was used to determine the Al flux (as a function of both Al and Cr gradients) in the γ phase at the γ/oxide interface. The COSP prediction, in effect, provided the information necessary to determine the Al concentration in the γ phase at the γ/oxide interface for each time iteration of the finite-difference calculation.

Model predictions provided an accurate description of the diffusional phenomena occurring in the coating and substrate during cyclic oxidation. A typical example of the predictive capability of the model is shown in the comparison of calculated concentration-distance profiles and those determined by electron microprobe analysis in Figure 3 for the Ni-10Cr substrate. The accuracy of the prediction at short time is somewhat hindered by the assumption of single-phase behavior; the accuracy at long times is hindered by the assumption of no variation in the type of oxide produced. Furthermore, significant variations of actual Al concentration-

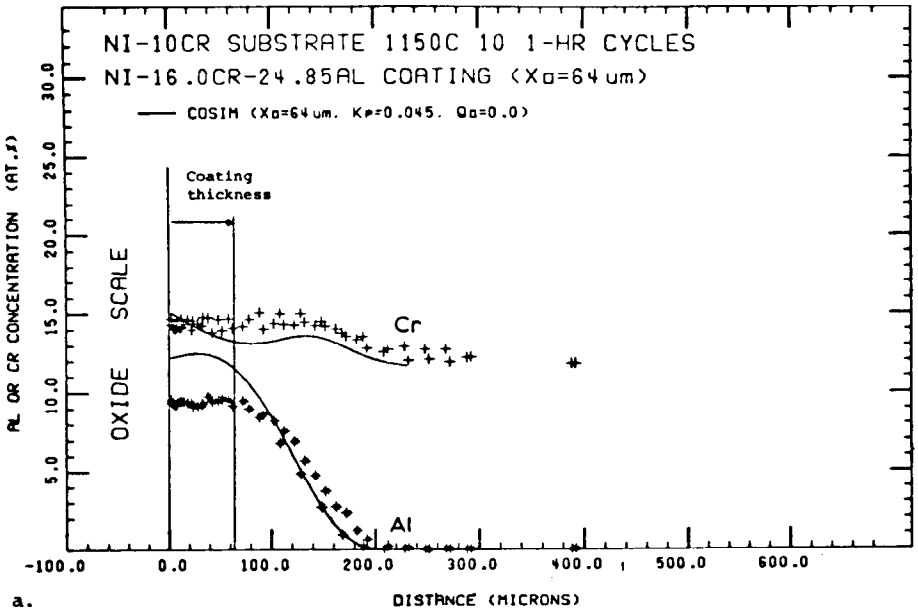

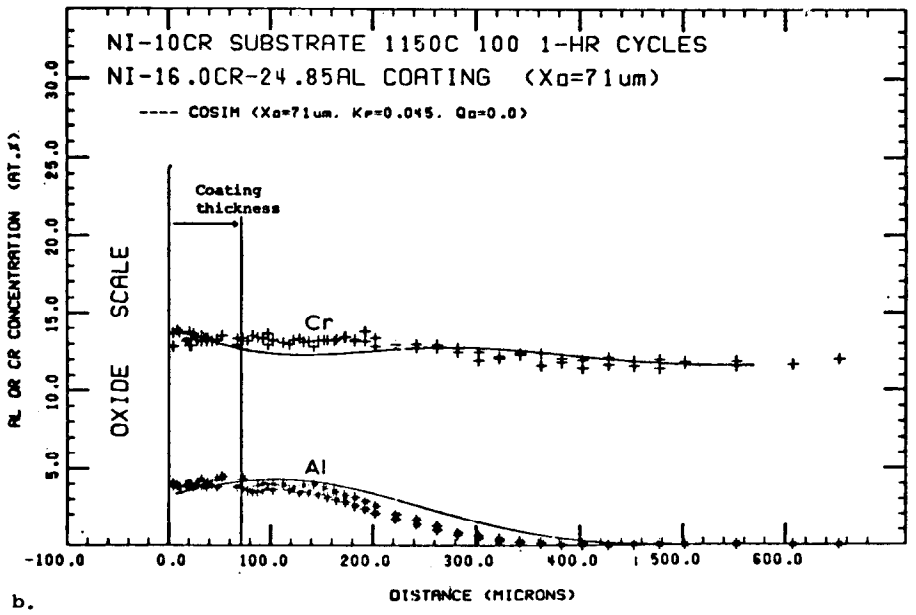

Figure 3. - Comparison of model-predicted (COSIM) and measured (electron microprobe analysis) concentration-distance profiles for oxidized, coated Ni-10Cr (a. 10 hours; b. 100 hours).

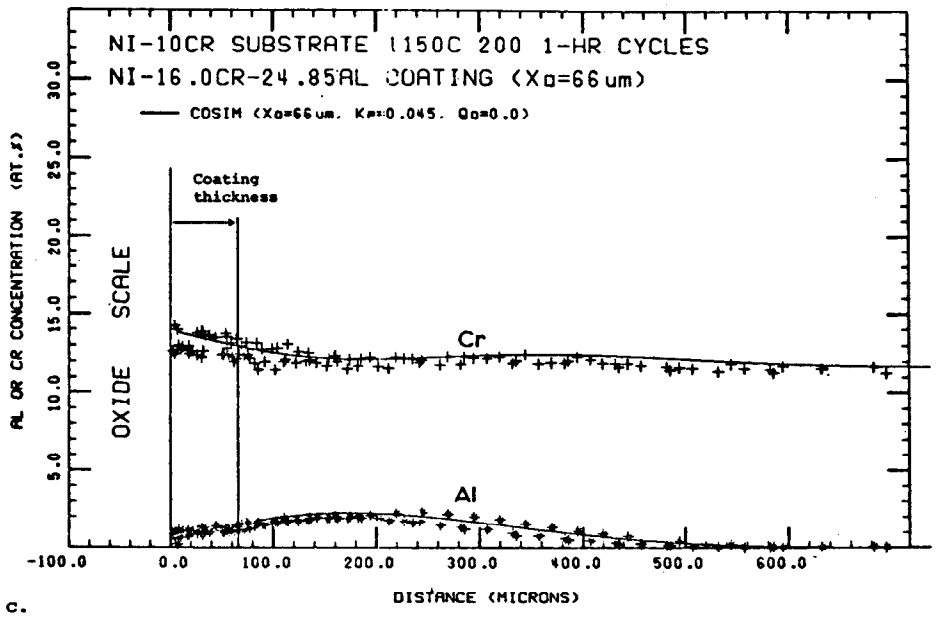

c.

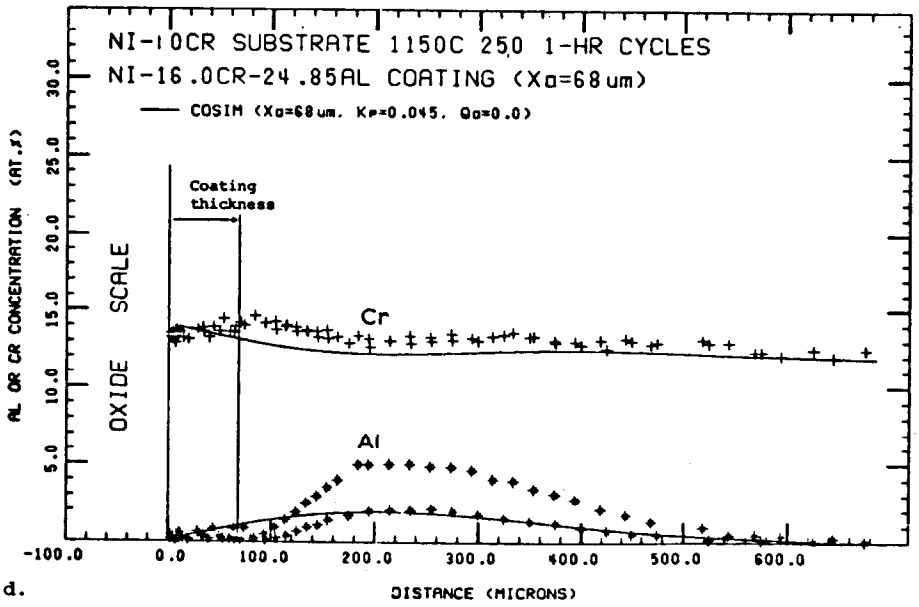

d.

Figure 3. - (continued) - (c. 200 hours, d. 250 hours).

distance profiles with position on the specimen can develop as the breakaway oxidation phenomena is approached with increasing time. It is noteworthy that the "bump" in the Cr profile often observed early in the diffusion sequence is accurately predicted by the model, and is the result of the Al gradient affecting Cr diffusion via the effect of D_{CrAl} and $\partial C_{Al}/\partial X$.

The predictive capability of the mathematical model permits its use as a tool to understand the general behavior of the cyclic oxidation of coated substrates for coating/substrate systems similar in behavior to those investigated experimentally in the present study. A wide variety of initial and boundary conditions were analyzed via the model in order to find the most and least significant parameters for high-temperature (1150°C) cyclic oxidation. Although a variety of model outputs were studied, attention will be directed to the time necessary for the Al concentration in the γ phase at the γ/oxide interface to reach zero, the theoretical life span of the coating as limited by breakaway oxidation. Clearly, the most dominant parameters on coating life are rate of Al consumption and Al concentration in the substrate, as shown in Figure 4. It should be noted that Al concentration in the coating has a lesser influence, for a given coating thickness, as shown in Figure 4b. However, the total amount of Al added via the coating (Al concentration in the coating multiplied by coating thickness) ranks as a major parameter as well. As might be anticipated, the concentration of Cr in either the alloy or the substrate exerts only a minor influence on the Al diffusion critical to the oxidation/degradation process.

The behavior of the Ni-13Cr-25Al-0.05Zr coating on $\gamma+\gamma'$ substrate alloys is the subject of ongoing investigations. Both Ni-Cr-Al ternary alloys (lower Cr and higher Al contents to form a series of alloys in the $\gamma+\gamma'$ field) and Mar-M 247-type alloys (with various Ta and C contents) are being explored in order for comparisons to the experimental studies and model results obtained for the same $\beta+\gamma$ coating on the γ-phase alloy substrates of Table I. Diffusion couples of the coating (in cast form) and the various $\gamma+\gamma'$ alloys are also being studied. Diffusion couples between the coating composition and ternary $\gamma+\gamma'$ alloys generally have larger bulk differences in Cr content than Al content. Two general results of this situation are: (a.) interdiffusion paths which pass through the $\beta+\gamma+\gamma'$ field, resulting in the formation of a γ'-phase layer between the $\beta+\gamma$ and $\gamma+\gamma'$ and (b.) growth of the $\beta+\gamma$ into the $\gamma+\gamma'$ (the $\beta+\gamma$ structure expands with time of interdiffusion). Couples between the coating composition and Mar-M 247-type alloys generally exhibit a γ-phase layer at the bond line; the layer grows with time at the expense of both the $\beta+\gamma$ and $\gamma+\gamma'$. Cyclic oxidation tests on coated Mar-M 247-type alloys indicate that the β phase is retained longer than in tests on coated specimens of the ternary γ-phase alloys. Variations in Ta content from about 1 atomic percent (normal Mar-M 247) down to zero resulted in significant variations in oxidation weight change with time. It is most interesting that these variations are apparent before the time of significant diffusional penetration of the Ta to the coating/oxide interface. In general, though, diffusional phenomena in $\beta+\gamma$/Mar-M 247 coating (or couple) systems appear to have many characteristics similar to $\beta+\gamma/\gamma$ systems, including maxima in Cr concentrations near the coating/substrate interface. Thus, this ongoing study gives promise of showing the applicability of the ternary diffusion oxidation model to the prediction of phenomena in actual coating/superalloy systems.

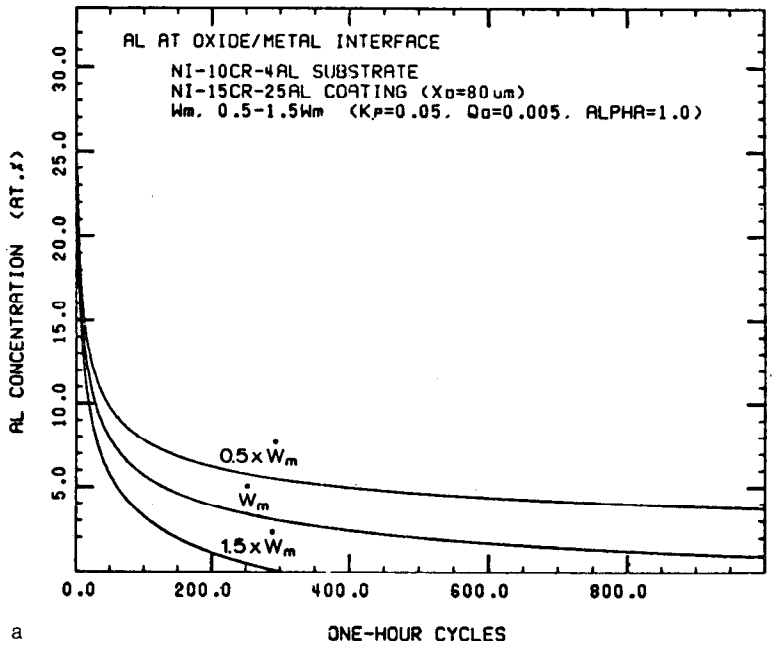

a

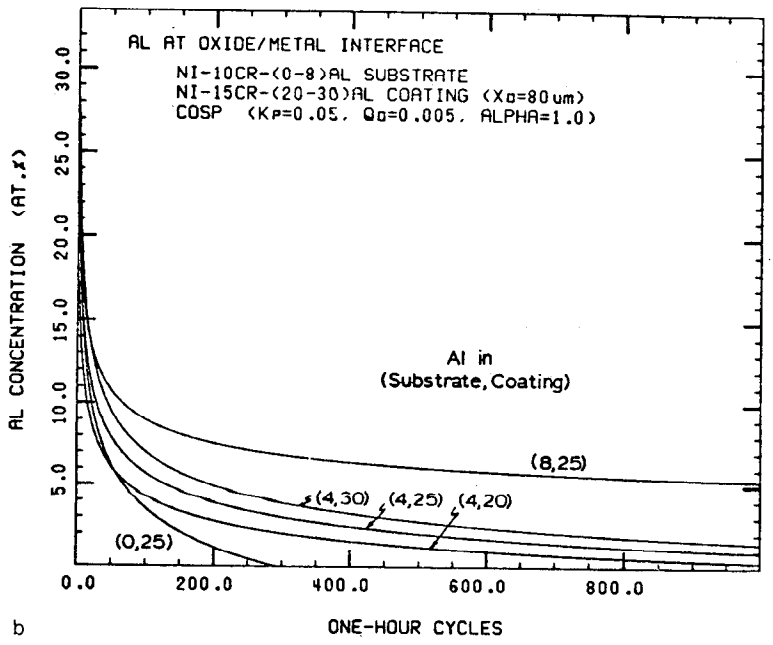

b

Figure 4. - Predicted effects of variations in Al consumption rate, $\dot{W}_m$, (top) and substrate and/or coating Al concentration (bottom) on the time-dependence of Al concentration in the γ phase at the γ/oxide interface.

Acknowledgements

The authors are grateful for numerous discussions with C. E. Lowell, S. R. Levine, C. A. Barrett and M. A. Gedwill of NASA-Lewis Research Center. In addition, their cooperation in supplying bulk alloys, powder for plasma spraying, some of the diffusion couples used in this study ($\gamma/\gamma+\gamma'$), chemical analyses, and cyclic oxidation testing facilities contributed significantly to the research. The authors are also grateful to M. R. Jackson of the General Electric Co. for numerous discussions and for the low-pressure plasma spraying of the various alloy substrates. The research was sponsored by NASA through grants NAG 3-244 and NAG 3-216.

References

1. G. W. Goward, "Protective Coatings for High-Temperature Alloys," pp. 369-386 in Source Book on Materials for Elevated Temperature Applications, American Society for Metals, Metals Park, OH, 1979 (also in Proceedings of the Symposium on Properties of High Temperature Alloys, Z. A. Foroulis and F. S. Pettit, eds.; Electrochemical Soc. Proceedings vol. 77-1, pp. 806-823, 1976).

2. S. Shankar, D. E. Koning and L. E. Dardi, "Vacuum Plasma Sprayed Metallic Coating," Journal of Metals, 33(10)(1981) pp. 13-20.

3. M. R. Jackson and J. R. Rairden, "Protective Coatings for Superalloys and the Use of Phase Diagrams," pp. 423-439 in Applications of Phase Diagrams in Metallurgy and Ceramics, G. C. Carter, ed.; NBS Spec. Publ. 496, National Bureau of Standards, Gaithersburg, MD, 1977.

4. W. K. Halman and D. Lee, "Electron Beam Physical Vapor Deposition Process for Coating Gas Turbine Airfoils," pp. 3-12 in High Temperature Protective Coatings, S. C. Singhal, ed.; TMS-AIME, Warrendale, PA, 1982.

5. M. Nakamori, Y. Harada and I. Hukua, "Evaluation of the High-Temperature Corrosion Resistance of Some Commercial Coatings and New Duplex Coatings for Gas Turbines," pp. 175-188 in High Temperature Protective Coatings, S. C. Singhal, ed.; TMS-AIME, Warrendale, PA, 1982.

6. C. J. Spengler, S. T. Scheirer and D. C. Barksdale, "Microstructural Characterization of Service Exposed CoCrAlY Overlay Coating," pp. 189-200 in High Temperature Protective Coatings, S. C. Singhal, ed.; TMS-AIME, Warrendale, PA, 1982.

7. J. A. Nesbitt and R. W. Heckel, "Solute Transport and the Prediction of Breakaway Oxidation in $\gamma+\beta$ Ni-Cr-Al Alloys," pp. 75-91 in High Temperature Protective Coatings, S. C. Singhal, ed.; TMS-AIME, Warrendale, PA, 1982.

8. J. A. Nesbitt, "Solute Transport During the Cyclic Oxidation of Ni-Cr-Al alloys," M.S. Thesis (available through University Microfilms, Ann Arbor, MI), Michigan Technological University, Houghton, MI, 1981 (also available as NASA Contractor Report No. 165544, May 1982).

9. K. E. Heinrich, R. L. Myklebust, H. Yakowitz and S. D. Rasberry, "A Simple Correction Procedure of Quantitative Electron Probe Microanalysis," NBS Technical Note 719, National Bureau of Standards, Gaithersburg, MD, 1972.

10. C. E. Lowell, C. A. Barrett and R. W. Palmer, "Development of a Cyclic Oxidation Spall Model," paper presented at the Oxidation, Deposition and Hot Corrosion in Combustion Turbine Engine Conference," NASA-Lewis Research Center, Cleveland, OH, April 1983.

11. J. S. Kirkaldy, "Isothermal Diffusion in Multicomponent Systems," pp. 55-100 in Advances in Materials Science, vol. 4, H. Herman, ed.; Interscience, New York, NY, 1970.

12. P. G. Shewmon, "Diffusion in Solids," pp. 28-32; McGraw-Hill, Inc., New York, NY, 1963.

13. D. P. Whittle and A. Green, "The Measurement of Diffusion Coefficients in Ternary Systems," Scripta Met., 8(7)(1974)pp. 883-884.

14. G. W. Roper and D. P. Whittle, "Analysis of Concentration Profiles Exhibiting Maxima and Minima," Scripta Met., 8(12)(1974) pp. 1357-1362.

15. R. F. Sekerka, C. L. Jeanfils and R. W. Heckel, "The Moving Boundary Problem," pp. 117-169 in Lectures on the Theory of Phase Transformations, H. I. Aaronson, ed.; TMS-AIME, Warrendale, PA, 1975.